

University of Groningen

Autophagy in normal hematopoiesis and leukemia

Folkerts, Hendrik

IMPORTANT NOTE: You are advised to consult the publisher's version (publisher's PDF) if you wish to cite from it. Please check the document version below.

Document Version

Publisher's PDF, also known as Version of record

Publication date:
2019

[Link to publication in University of Groningen/UMCG research database](#)

Citation for published version (APA):

Folkerts, H. (2019). *Autophagy in normal hematopoiesis and leukemia: Biological and therapeutic implications*. [Thesis fully internal (DIV), University of Groningen]. Rijksuniversiteit Groningen.

Copyright

Other than for strictly personal use, it is not permitted to download or to forward/distribute the text or part of it without the consent of the author(s) and/or copyright holder(s), unless the work is under an open content license (like Creative Commons).

The publication may also be distributed here under the terms of Article 25fa of the Dutch Copyright Act, indicated by the "Taverne" license. More information can be found on the University of Groningen website: <https://www.rug.nl/library/open-access/self-archiving-pure/taverne-amendment>.

Take-down policy

If you believe that this document breaches copyright please contact us providing details, and we will remove access to the work immediately and investigate your claim.

Downloaded from the University of Groningen/UMCG research database (Pure): <http://www.rug.nl/research/portal>. For technical reasons the number of authors shown on this cover page is limited to 10 maximum.

06.

**Elevated VMP1 expression in acute
myeloid leukemia amplifies autophagy
and is protective against venetoclax-
induced apoptosis**

H. Folkerts, A.T.J. Wierenga, F.A.J. van den Heuvel,
R.R. Woldhuis, D.S. Kluit, J. Jaques, J.J. Schuringa, E. Vellenga

Submitted

Abstract

Vacuole membrane protein (VMP1) is a putative autophagy protein, which together with Beclin-1 acts as a molecular switch in activating autophagy. In the present study the role of VMP1 was analysed in CD34⁺ cells of cord blood (CB) and primary acute myeloid leukemia (AML) cells and cell lines. An increased expression of VMP1 was observed in a subset of AML patients. Functional studies in normal CB CD34⁺ cells indicated that inhibiting VMP1 expression reduced autophagic-flux, coinciding with reduced expansion of HSPC, delayed differentiation, increased apoptosis and impaired in vivo engraftment. Comparable results were observed in leukemic cell lines and primary AML CD34⁺ cells. Ultrastructural analysis indicated that leukemic cells overexpressing VMP1 displayed a reduced number of mitochondrial structures, while the number of lysosomal degradation structures was increased. The overexpression of VMP1 did not affect cell proliferation and differentiation, but increased autophagic-flux and improved mitochondrial quality, which coincided with an increased threshold for venetoclax-induced loss of mitochondrial outer membrane permeabilization (MOMP) and apoptosis. In conclusion, our data indicate that in leukemic cells high VMP1 is involved with mitochondrial quality control.

Introduction

Macroautophagy (referred to as autophagy) is a multi-step catabolic process involved in lysosomal degradation of redundant cellular constituents, such as organelles and proteins (1-3). Autophagy is essential for hematopoietic stem cell (HSC) maintenance, in part by actively limiting mitochondrial oxidative metabolism (4,5). During HSC differentiation the autophagic-flux gradually declines, but autophagy might have distinct functions in terminal differentiated cells (6). It controls the clearance of mitochondria in erythroid precursor cells and is essential for monocyte-to-macrophage differentiation (7-10). For the malignant counterpart, studies have shown that a subgroup of AML cells heavily relies on autophagy for their survival (11-13), whereby increased autophagy is associated with therapy resistance (14-18). The increased autophagy is observed especially in poor-risk AML (11). Since mutations in autophagy genes have only been observed in the minority of patients (19), increased autophagy is most likely related to other phenomena, such as therapy-induced changes in their metabolism. Inhibition of autophagy by knockdown of essential autophagy genes such as ATG5 or ATG7 impairs AML *in vitro* cell proliferation and *in vivo* engraftment (11,16,20). This vulnerability relies on accumulation of (dysfunctional) mitochondria, as evident by the increased reactive oxygen species (ROS) production and the activation of p53-mediated apoptosis (11).

Vacuole membrane protein (VMP1) is additional autophagy protein residing in the endoplasmic reticulum (ER) membrane (21,22), which can interact with the BH3 domain of Beclin-1, thereby activating autophagy (23). The anti-apoptotic BCL-2 family members can also bind to the BH3 domain of Beclin-1, resulting in the dissociation of VMP1 and subsequent inhibition of the autophagic-flux (23,24). Little information is available on VMP1 in hematopoietic cells, but in solid tumours it has been shown that VMP1-dependent autophagy can be activated under stress conditions such as starvation and hypoxia (25,26). We therefore determined whether VMP1 is essential for autophagy in normal and malignant hematopoiesis and whether high VMP1 expression provides survival benefits for leukemic cells.

The results showed that VMP1 is important for survival of normal hematopoietic stem cells and progenitor (HSCP) cells *in vitro* and *in vivo*. Moreover, VMP1 expression was significantly increased in AMLs. Overexpression studies and ultrastructurally analysis revealed that VMP1 is involved in mitochondrial quality

control, thereby protecting cells against oxidative stress. We concluded that high VMP1 expression increases autophagic flux and the threshold for venetoclax-mediated loss of MOMP and thereby reducing apoptosis-mediated cell death.

Material and Methods

Isolation and culture of human CD34⁺ cells

Umbilical cord blood (UCB) obtained from full-term healthy neonates who were born at the Obstetrics departments of the Martini Hospital and the University Medical Center Groningen (Groningen, the Netherlands) after informed consent. AML blasts derived from peripheral blood cells or bone marrow were obtained from patients in accordance with the Declaration of Helsinki; the protocols were approved by the Medical Ethics Committee of the University Medical Center Groningen (UMCG). Mononuclear cells (MNC) were isolated from UCB, or peripheral blood or bone marrow from AML patients by Ficol density centrifugation, and CD34⁺ cells were subsequently isolated with the autoMACS pro-separator (Miltenyi Biotec, Amsterdam, the Netherlands). AML patient characteristics are indicated in **supplemental Table S1**.

Cell culture

Primary AML, normal bone marrow or CB-derived CD34⁺ cells were cultured in suspension or in T25 flasks pre-coated with MS5 stromal cells in Gartners medium: Alpha-MEM (Lonza, Leusden, the Netherlands) supplemented with 12.5% FCS and 12.5% Horse serum (Sigma-Aldrich, Saint Louis, USA), 1% penicillin/streptomycin (PAA Laboratories, Dartmouth, USA), 1 μ M hydrocortisone (Sigma-Aldrich), 57.2 μ M beta-mercaptoethanol and cytokines: G-CSF, Human TPO agonist; Romiplostim (Amgen, Breda, the Netherlands) and IL-3 (20 ng/mL each) (27). The relative increase in Cyto-ID signal after overnight incubation with 20 μ M hydroxychloroquine (HCQ) was defined as the autophagy flux (6,11). The concentration and incubation time of HCQ for measuring autophagic-flux was validated and is based on maximal accumulation of autophagosomes, without affecting cell viability, after overnight incubation with HCQ (6,11). The leukemic cell lines HL60, OCIM3, MOLM13 and THP1 were obtained from ATCC and the cell lines were all tested mycoplasma free by PCR. All leukemic cell lines cells were cultured in RPMI 1640, supplemented with 10% FCS and 1% penicillin/streptomycin.

Antibodies and reagents

The following anti-human antibodies were used: mouse anti-SQSTM1/p62 (sc-28359) and rabbit (sc-130656) or mouse (sc-47778) anti-Actin, from Santa Cruz (Santa Cruz, CA, USA), Mouse anti-LC3 (5F10, 0231-100) from Nanotools (Munich, Germany), P62, and anti-BCL-2 (Santa Cruz, CA, USA), anti-TOM20 and anti-VMP1 were obtained from cell signalling (Leiden, the Netherlands), Hydroxychloroquine (HCQ), was obtained from Sigma-Aldrich. Venetoclax / ABT-199 (BCL-2 inhibitor, Selleckchem Munich, Germany), S63845 (MCL-1 inhibitor) was obtained from APEX BIO (Boston, MA, USA).

Mitochondrial copy number assay

Total DNA was isolated from $>1 \times 10^5$ cells using RNeasy mini kit (Qiagen, Venlo, the Netherlands). Obtained total DNA was real-time amplified in iQ SYBR Green Supermix (Bio-Rad) with the CFX connect Thermocycler (Bio-Rad). The nuclear genes GAPDH and B2M or mitochondrial genes 12S and tRNA were amplified. The obtained CT values were corrected for the corresponding calculated primer reaction efficiencies. Based on the corrected CT values, the mtDNA copy number was calculated relative to nuclear DNA copy number (28). The primer sequences are listed in the **Supplemental Table S2**.

Virus production and transduction of CD34⁺ leukemic cells or cell lines

Five lentiviral plasmids with short hairpin RNA (shRNA) targeting Vacuole Membrane Protein 1 (VMP1) were obtained from GE Healthcare Dharmacon. The shRNAs were cloned into a pLKO.1-mCherry lentiviral vector using MunI & SacII restriction enzymes (Thermo Scientific). After initial testing, two shRNAs (Clone ID TRCN0000135158 and TRCN0000138386) were selected for this study based on effective knockdown efficiency. A shRNA sequence that does not target human genes (referred to as scrambled) was used as a control. Lentiviral virions were produced by transient transfection of HEK 293T cells with pCMV and VSV-G packaging system using Polyethylenimine (Polyscience Inc. Eppelheim, Germany) or FuGENE (Promega, Leiden, the Netherlands). Retroviral virions containing pBABE-puro-mCherry-EGFP-LC3B were produced as described earlier (11). Viral supernatants were collected and filtered through a 0.2- μ m filter and subsequently concentrated using Centriprep Ultracel YM-50 centrifugal filters (Millipore, Amsterdam, The Netherlands). CD34⁺ cells were seeded in Gartners medium supplemented with cytokines (specified previously). Transduction was performed by adding 0.5 mL of ~10 times concentrated viral supernatant to 0.5 mL of medium

containing 0.5×10^6 cells in the presence of 4 $\mu\text{g}/\text{mL}$ polybrene (Sigma-Aldrich).

ATP assay

Luminescent ATP Detection Assay Kit (Abcam, Cambridge, UK, ab113849) was used to measure the levels of ATP, according to the manufacturer's protocol.

Gene ontology (GO) analysis in AML

Publicly available data of two large AML expression datasets with 460 (GSE6891 (29)) and 173 (TCGA dataset (30)) samples, respectively, was analysed using the R2 Genomics Analysis and Visualization Platform (<http://r2.amc.nl>). Gene expression data of all genes was correlated with VMP1 expression. Correlations with a p-value of $\geq .01$ and/or with a correlation coefficient of $r = \leq .25$ were discarded. Next, genes which positively or inversely correlated with VMP1 expression in both AML datasets were compared. In total 551 (26.8% overlap) positively correlating genes and 979 (24.1% overlap) inversely correlating genes were present in both datasets. Gene ontology analysis, using David (31), was performed on the overlapping positively or inversely correlating genes.

Electron microscopy

The experimental procedure for ultrastructural analysis of hematopoietic cells has been described previously (32). In brief, FACS sorted OCIM3 cells transduced with pRRL-blueberry or pRRL-VMP1-blueberry and OCIM3 cells transduced with shSCR-mCherry or shVMP1-mCherry were pelleted and subsequently fixed in 2% paraformaldehyde and 2% glutaraldehyde in 0.1M cacodylate buffer for 24 hrs at 4°C. After fixation the cells were washed in 0.1M cacodylate buffer. Cells were stained with Evans blue and subsequently embedded in low melting point agarose, as described previously (33). Agarose pieces containing the cell pellet were dehydrated, osmicated, and embedded in Epon according to routine procedures. Semi-thin sections (0.5 μm) stained with toluidine blue were inspected using light microscopy to select for OCIM3 cells. Ultra-thin sections (60-80 nm) were cut and stained with 4% uranyl acetate in water, followed by Reynolds lead citrate. Images were taken with a Zeiss Supra55 in STEM (Oberkochen, Germany) mode with ATLAS software developed by Fibics (Ottawa, Ontario, Canada) and the CM100 (Eindhoven, the Netherlands).

***In vivo* transplantations into NSG mice**

Twelve- to thirteen -week-old female NSG (NOD.Cg-Prkdcscid IL2rgtm1WjL/SzJ)

mice were purchased from the Central Animal Facility breeding facility within the UMCG. Mouse experiments were performed in accordance with national and institutional guidelines and all experiments were approved by the Institutional Animal Care and Use Committee of the University of Groningen (IACUC-RuG). The experiment was performed as described previously (6).

Statistical analysis

An unpaired two-sided Student's t-test or a Mann Whitney U test was used to calculate statistical differences. A p-value of <.05 was considered statistically significant.

Results

VMP1 expression is increased in a subset of CD34⁺ AML cells

We previously performed transcriptome analysis on a publicly available gene expression database of normal HSPCs and AML cells (Bloodspot expression database, (34)) with a focus on autophagy associated genes. This showed that several core-autophagy genes were differentially expressed in AML compared to normal HSPCs (11). Further analysis revealed that putative autophagy protein VMP1 was expressed at significantly higher levels in AMLs compared to normal HSPCs (**Figure 1A**). In contrast, the expression of known VMP1 interaction protein Beclin-1 was not different between AML and normal HSPCs (**Figure 1A**). The elevated expression of VMP1 was validated by quantitative polymerase chain reaction (qPCR), whereby the highest VMP1 expression was observed in CD34⁺ AMLs with a monocytic phenotype (**Figure 1B**). Western blot analysis of VMP1 confirmed variable protein levels of VMP1 in primary AML CD34⁺ cells (**Figure 1C**), whereby VMP1 mRNA levels significantly correlated with VMP1 protein levels ($R=0.6801$, $p<.01$, **Figure 1D**). Together these findings indicate that VMP1 is overexpressed in a subset of primary AML CD34⁺ cells.

VMP1 knockdown in HSPCs results in inhibition of autophagy and an impaired *in vitro* expansion and *in vivo* engraftment.

To investigate the functional role of VMP1 in HSPCs and their progeny, human CB-derived CD34⁺ cells were transduced with lentiviral shRNAs targeting VMP1 and subsequently cultured *in vitro* or transplanted *in vivo* (**Figure 2A**). A panel of five shRNAs was tested, of which two were selected. Knockdown of VMP1

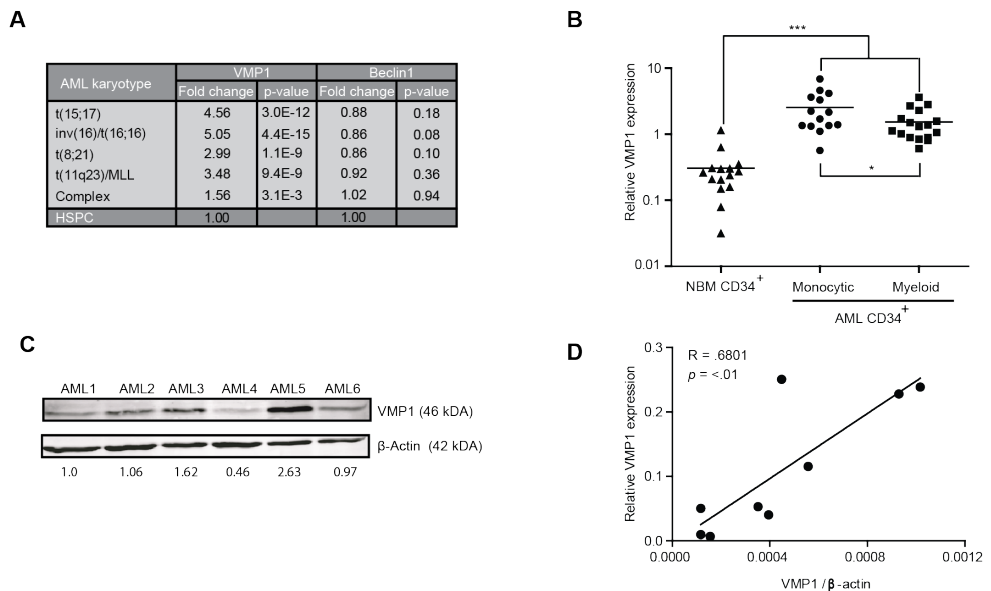


Figure 1. VMP1 expression is increased in a subset of AMLs. A) Expression of VMP1 and Beclin-1 in mononuclear primary AML cells acquired from the publicly available expression dataset Bloodspot. HSPC is defined as the combined fractions of HSC, MMP, CMP, GMP and MEP. **B)** Gene expression of VMP1 determined by quantitative RT-PCR in normal bone marrow (NBM) CD34⁺ cells (n=15), AMLs with myeloid (n=17) or monocytic characteristics (n=14). **C)** Western Blot showing variation in VMP1 protein levels in different AMLs, beta-actin was used as control and VMP1 / beta-actin levels are shown relative to AML1. **D)** Correlation between VMP1 mRNA levels and protein levels in primary AML CD34⁺ cells (n=9). Error bars represent SD; * or *** represents $p < .05$ or $p < .001$, respectively.

in CB CD34⁺ cells was confirmed at the mRNA and protein level with both shVMP1#1 and shVMP1#2 (**Figure 2B**). Knockdown of VMP1 resulted in inhibition of the autophagic-flux as determined by relative accumulation of Cyto-ID after HCQ treatment at day 7 during both myeloid and erythroid liquid cultures (**Supplemental Figure S1A**). As reported previously (6), the autophagic-flux was higher under erythroid- compared to myeloid-culture conditions (**Supplemental Figure S1A**). A significant reduction in erythroid progenitor (BFU-E) frequency was observed in *in vitro* colony assays upon knockdown of VMP1 (**Figure 2C**), while no change in myeloid colony formation was observed. However, a reduction in relative expansion was observed upon knockdown of VMP1 under both erythroid and myeloid culture conditions (**Figure 2D**).

To assess whether VMP1 knockdown would affect the differentiation potential of CB CD34⁺ cells the expression of myeloid (CD14, CD15) and erythroid differentiation markers (CD71, CD235A) were analysed using flow cytometry. This

revealed only a minor delay in CD14 expression at day 8 (**Supplemental Figure S1B**), but a stronger effect on terminal erythroid differentiation (**Supplemental Figure S1C**). To study the long-term effects of VMP1 knock-down in the context of the micro-environment, transduced CD34⁺ HSPCs were cultured in MS5 bone marrow stromal co-cultures, in which VMP1 knockdown resulted in reduced expansion, as determined by the decline in percentage of mCherry positive cells (**Supplemental Figure S1D**). The negative phenotype of shVMP1-transduced HSPCs was at least in part caused by increased apoptosis (**Supplemental Figure S1E**), while cell cycle progression was not affected (**Supplemental Figure S1F**). To assess whether VMP1 knockdown also affected *in vivo* engraftment, unsorted shSCR or shVMP1-mCherry-transduced CB CD34⁺ cells were transplanted into immunodeficient NSG mice (**Figure 2A**). Transplanted CD34⁺ cells were ~60% mCherry-positive. Engraftment, as determined by the percentage huCD45

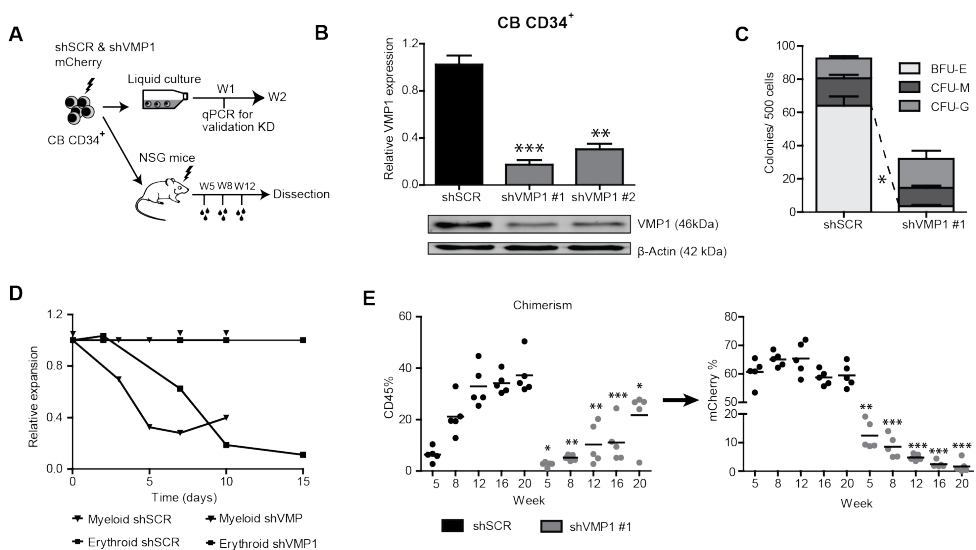


Figure 2. VMP1 knockdown in HSPCs results in inhibition of autophagy and an impaired *in vitro* expansion and *in vivo* engraftment. **A**) Experimental scheme, shSCR-mCherry or shVMP1-mCherry transduced cord blood (CB) CD34⁺ cells were cultured *in vitro* under myeloid or erythroid liquid culture conditions or injected IV in sub-lethally irradiated NSG mice. Bleeds were performed at week 5, 8 and 12 after injection and analysed by FACS. **B**) Knockdown efficiency of VMP1 was determined by quantitative RT-PCR and Western blotting of CB CD34⁺ cells transduced with shSCR, shVMP1 #1 or shVMP1 #2. **C**) CFC assay with freshly sorted shSCR or shVMP1 #1 transduced CB CD34⁺ cells (n=2). **D**) Representative graph showing relative expansion of shVMP1 transduced CB CD34⁺ cells under myeloid or erythroid permissive liquid culture conditions, shSCR transduced cells were used as control (n=2). **E**) Percentage of engraftment represented by huCD45 percentage (left graph) and the percentage mCherry within the huCD45⁺ population (right graph). Each dot represents data from a single mouse, n=5 for each group. Error bars represent SD; *, ** or *** represents p<.05, p<.01 or p<.001, respectively.

in peripheral blood, was significantly reduced in shVMP1 mice compared to controls (**Figure 2E**, left panel). While mCherry levels for shSCR remained stable around ~60%, the contribution of the shVMP1 transduced cells to the engrafted cells over time was significantly reduced (**Figure 2E**, right panels). At sacrifice, high engraftment levels in bone marrow, spleen and liver were observed, and the contribution of shSCR-mCherry transduced cells within the CD45 compartment was around ~60% in all analyzed organs (**Supplemental Figure S1G**, left panel). In contrast, the percentage of shVMP1-mCherry transduced cells within the CD45 compartment was strongly reduced (**Supplemental Figure 1G**, right panel). Together these findings indicate that knockdown of VMP1 inhibits autophagic-flux and results in reduced expansion of HSPC, delayed differentiation and an impaired long-term engraftment *in vivo*.

VMP1 knockdown results in inhibition of autophagy, impaired expansion, increased apoptosis and reduced cell cycle progression in leukemic cells.

Because VMP1 was shown to be differentially expressed in leukemia (**Figure 1**), the consequences of VMP1 modulation were assessed in leukemic cells. First, leukemic cell lines expressing variable levels of VMP1 were transduced with shVMP1 or shSCR lentivectors and knockdown efficiencies were confirmed at the protein level, while BCL-2 levels were not affected (**Figure 3A**). Knockdown of VMP1 was associated with impaired autophagy, reflected by accumulation of SQSTM1/p62 (**Figure 3A**) and reduced accumulation of LC3 puncta after HCQ treatment (35) (**Figure 3B**, **Supplemental Figure S2A**). The knockdown of VMP1 had a strong impact on cell growth (**Figure 3C**), which was at least in part due to increased apoptosis, as determined by annexin-V positivity (**Figure 3D**). In addition, cell cycle analysis showed that cells accumulated in G1 phase significantly (**Figure 3E**). Next, AML patient-derived CD34⁺ (n=3) cells were transduced with shVMP1-mCherry or shSCR-mCherry. The unsorted cells were cultured long-term in MS5 bone marrow stromal cocultures. The transduction efficiency in AML CD34⁺ cells was between 20-60% and was comparable between shSCR and shVMP1 within a single AML sample (**Supplemental Figure S2B**). Similar to leukemic cell lines, knockdown of VMP1 resulted in decreased expansion of primary AML CD34⁺ cells, relative to scrambled control (**Figure 3F**). Together, these results indicate that VMP1 is essential for survival and proliferation of leukemic cell lines and patient-derived AML CD34⁺ cells.

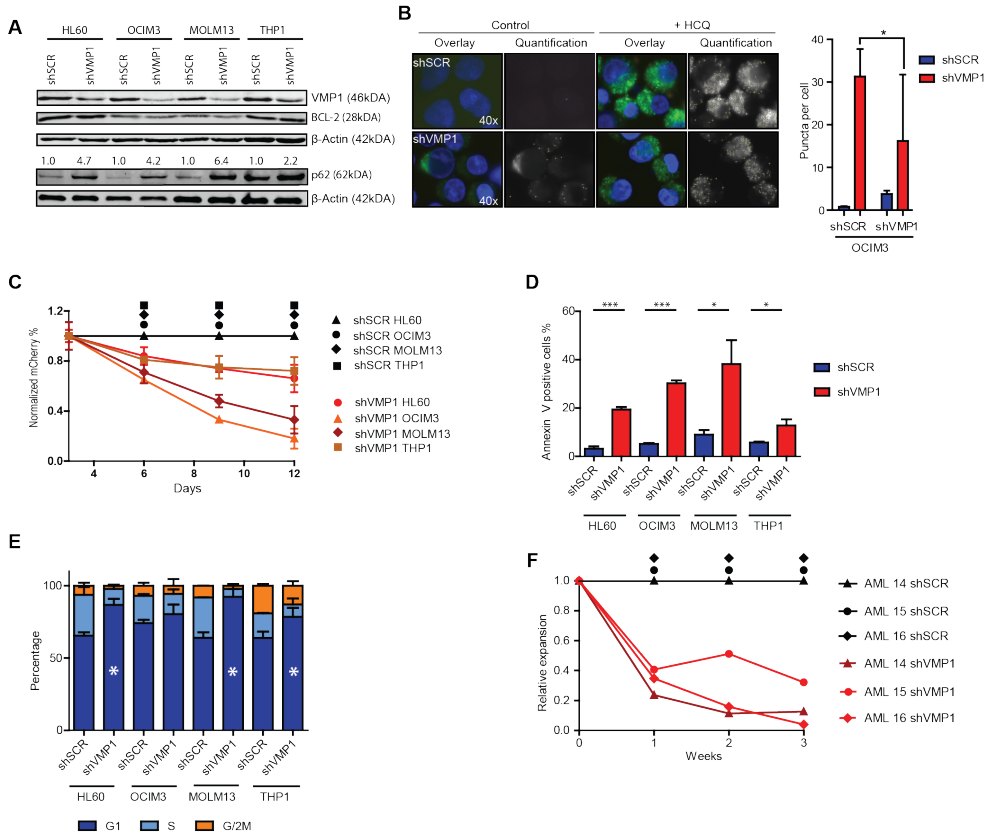


Figure 3: VMP1 knockdown results in inhibition of autophagy, impaired expansion, increased apoptosis and reduced cell cycle progression in leukemic cells. A) Western blot analysis of VMP1, BCL-2 and p62/SQSTM1 protein levels after knockdown of VMP1, beta-actin was used as control. **B)** Left panel, representative pictures showing GFP-LC3 puncta in shSCR or shVMP1 transduced OCIM3 cells treated with or without HCQ. Right panel, quantification of LC3 puncta. **C)** Cell growth in time of shSCR or shVMP1 transduced leukemic cell lines; HL60, OCIM3, MOLM13 and THP1 (n=3). **D)** Graph showing percentage of annexin-V positive cells of shSCR or shVMP1 transduced leukemic cell lines (n=3). **E)** Cell cycle analysis after Hoechst staining of shSCR or shVMP1 transduced leukemic cells (n=2). The * in G1-phase of shVMP1 transduced leukemic cell lines indicates a significant difference compared to shSCR control. **F)** Relative expansion of AML CD34⁺ cells after knockdown of VMP1 (n=3) cultured on a MS5 stromal layer. shSCR transduced AML CD34⁺ cells were used as control. Error bars represent SD; *, ** or *** represents p<.05, p<.01 or p<.001, respectively.

Overexpression of VMP1 increases autophagic-flux in leukemic cells and is involved in mitochondrial turnover.

To study the consequences of high expression of VMP1 on normal and leukemic hematopoietic cells, a lentiviral VMP1-Blueberry overexpression vector (VMP1-OE) was constructed, and overexpression of VMP1 was confirmed at the protein level (**Figure 4A**). Overexpression resulted in reduced p62/SQSTM1 protein

levels, indicating increased autophagy activity. (**Figure 4A**). Next, leukemic cell lines expressing the mCherry-GFP-LC3 autophagy reporter were transduced with control or VMP1-OE cells to assess the impact on the autophagy flux. An increased mCherry/GFP ratio was observed in OCIM3 and THP1 cells overexpressing VMP1, confirming that the autophagy-flux was increased (**Figure 4B-C**). The increased autophagy did not affect the cell proliferation of the cell lines.

To obtain more insight into the role of VMP1 in AML, two large AML expression datasets (29,30) were analysed using the R2 Genomics Analysis and Visualization Platform. Gene ontology analyses (GO) was performed on genes correlating with VMP1 expression. GO analysis revealed that positively correlated genes were enriched for the GO terms lysosome, vacuole and vesicle transport, while inversely correlated genes were enriched for the GO terms mitochondrion, DNA replication, ATP binding, apoptosis and cell cycle (**Figure 4D**). Because high VMP1 expression in AML cells is inversely correlated with gene signatures associated with mitochondria (**Figure 4D**, right panel), mitochondrial function was assessed

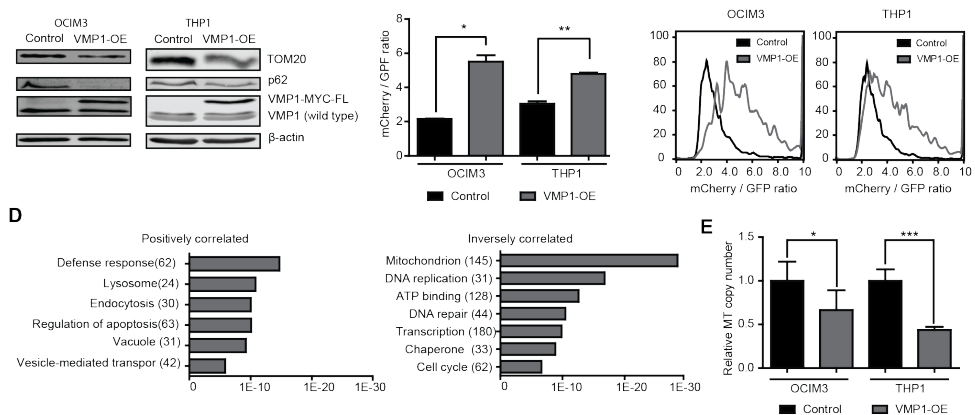


Figure 4. Overexpression of VMP1 increases autophagic-flux in leukemic cells and is involved in mitochondrial turnover. **A**) Western blot analysis of TOM20, p62 and VMP1 in OCIM3 and THP1 cells overexpressing VMP1 (VMP1-OE) or control. **B**) The mCherry / GFP ratio determined in mCherry-GFP-LC3 expressing leukemic cell lines, transduced with control or VMP1 OE. **C**) Representative FACS of the mCherry/GFP ratio analysis in OCIM3 and THP1 cells. **D**) Gene ontology analysis (David) was performed on two large AML patient gene expression datasets. Figures showing p-values of enriched gene sets, positively (left graph) or inversely (right graph) correlated with VMP1 expression in AMLs. **E**) Mitochondrial copy number in OCIM3 and THP1 cells with VMP1-OE or control. Error bars represent SD; * or ** represents $p < .05$ or $p < .01$, respectively.

after modulation of VMP1 expression. Overexpression of VMP1 led to a significant decrease in mitochondrial DNA (mtDNA) copy number relative to nuclear DNA (nucDNA) in OCIM3 and THP1 cells (**Figure 4E**). In line with these results, TOM20 which is a marker for mitochondrial mass, was decreased after overexpression of VMP1 (**Figure 4A**). Conversely, shVMP1 transduced leukemic cells had an increase in mtDNA copy number in cell lines. (**Supplemental Figure S3A**). However, this increase was not observed in MOLM13 cells. Together these findings indicate that overexpression of VMP1 is involved in mitochondrial turnover.

Ultrastructural analysis and mitochondrial function in OCIM3 cells after VMP1 modulation

To obtain more insight into the involvement of VMP1 in mitochondrial quality control, we analyzed OCIM3 cells ultrastructurally with electron microscopy (EM) after lentiviral overexpression or knockdown of VMP1. OCIM3 cells overexpressing VMP1 displayed a reduction in the number of mitochondrial structures compared to control cells (**Figure 5A**, $p < .01$). Representative ultrastructural images are shown in Figure 5B. In the shVMP1-transduced OCIM3 cells mitochondria were on average ~24% larger and swollen compared to control (**Supplemental Figure 4A**). Moreover, in contrast to VMP1-OE, cells with knockdown of VMP1 had elevated numbers of mitochondrial structures (**Figure 5C-D**, $p < .05$). In addition, the mitochondrial function was analyzed after VMP1 modulation. The mitochondrial membrane potential (MMP) measured by tetramethylrhodamine (TMRM) was significantly increased in OCIM3 cells overexpressing VMP1, while there was a trend for reduced MMP upon VMP1 knockdown (**Figure 5E**). Although the number of mitochondria in VMP1 overexpressing cells was reduced (**Figure 4**), these cells had higher levels of ATP content (**Figure 5F**). Conversely, knockdown of VMP1 resulted in decreased ATP production with concomitant increased ROS levels, indicating a loss in mitochondrial function (**Figure 5F**, **Supplemental Figure S4B-C**). Additional analysis by EM revealed that cells overexpressing VMP1 had an increased number of onion-like multilamellar membrane structures, also called whorls (**Figure 5A** and **5G**, 1.5 fold, $p < .05$). These structures are associated with lysosomal mediated degradation of intra-cellular parts, also termed the degradative compartment (36), and are associated with an increased autophagy flux. Together, the increase in autophagy, the reduced number of mitochondria structures in response to VMP1 overexpression are indicative of increased turnover of mitochondria.

Figure 5.

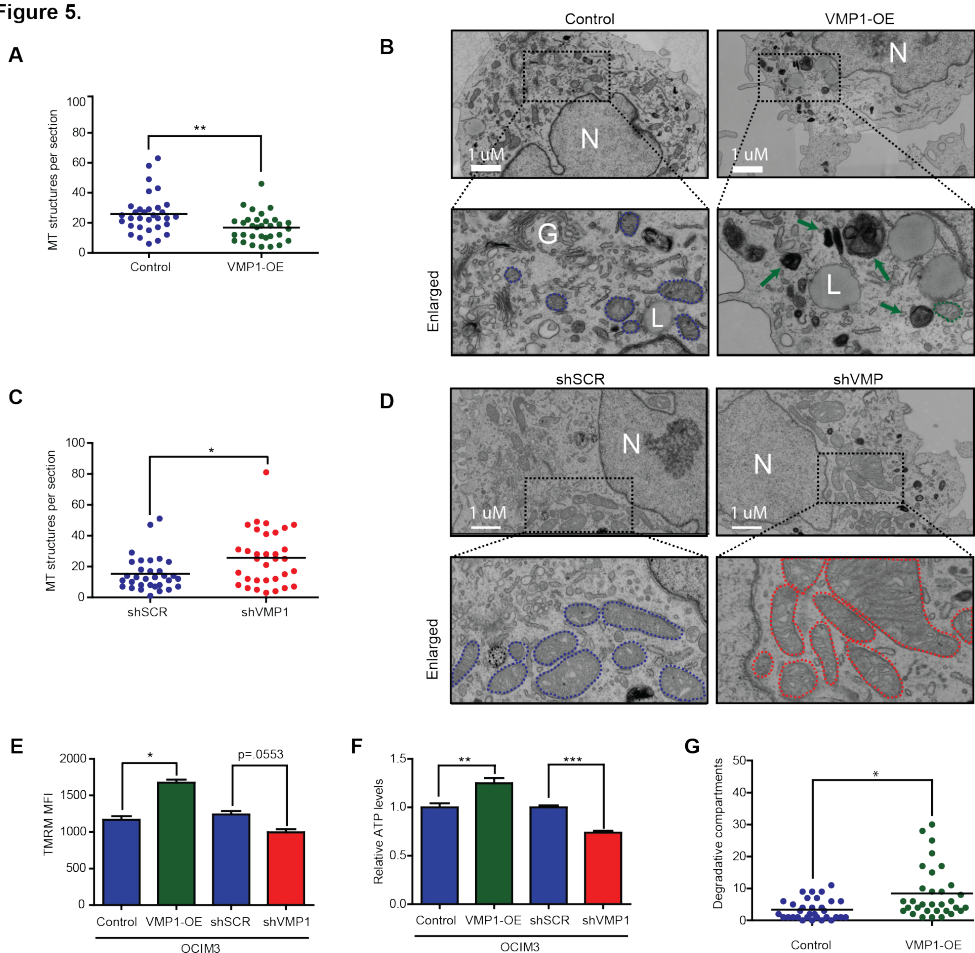


Figure 5. Ultrastructural analysis and mitochondrial function in OCIM3 cells after VMP1 modulation. **A**) Quantification of mitochondrial structures per section in OCIM3 cells transduced with lentiviral vectors for overexpression of VMP1 (VMP1-OE) or control ($n > 32$ sections per group). **B**) Representative ultrastructural pictures of OCIM3 cells overexpressing VMP1 or control. N = nucleus, L = lipid droplet, G = Golgi, green arrow = whorls/degradative compartments. The blue (control) or green (VMP1-OE) dotted lines indicate mitochondrial structures. **C**) Quantification of mitochondrial structures per section in OCIM3 cells with knockdown of VMP1 (shVMP1) or control vectors ($n > 32$ sections per group). **D**) Representative ultrastructural pictures of OCIM3 cells with knockdown of VMP1 or control. N = nucleus. The blue (control) or red (shVMP1) dotted lines indicate mitochondrial structures. **E**) FACS analysis of mitochondrial membrane potential (MMP) after tetramethylrhodamine (TMRM) staining in OCIM3 with VMP1 overexpression, VMP1 knockdown or control ($n = 3$). **F**) ATP levels measured in OCIM3 with VMP1 overexpression, VMP1 knockdown or control ($n = 4$). **G**) Electron microscopy, quantification of onion-like multilamellar membrane structures called degradative compartments per section of OCIM3 cells, transduced with VMP-OE or control ($n \leq 35$ cells per group). Examples of degradative compartments are indicated by green arrows in **Figure 5B** right panels. Error bars represent SD; * or ** represents $p < 0.05$ or $p < 0.01$ respectively.

Overexpression of VMP1 interferes with venetoclax induced apoptosis.

BCL-2 protein family members regulate apoptosis by controlling the permeability of mitochondria (37). Interestingly, VMP1 has been shown to contain a BH3-binding domain, which is an important characteristic of the BCL-2 protein family (38). The specific BCL-2 inhibitor venetoclax has been shown to disrupt the BH3 dependent BCL-2/Beclin-1 interaction, thereby activating autophagy (39,40). First, we studied the consequences for autophagy activity after venetoclax treatment in the context of high VMP1 expression. As expected, in THP1 cells p62 levels declined in a dose-dependent manner with increasing concentration of venetoclax, which is indicative for increased autophagic-flux (Figure 6A). Basal p62 levels were reduced in THP1 cells overexpressing VMP1, while p62 levels further declined with increasing concentrations of venetoclax (Figure 6A). Next, we evaluated the effect of high VMP1 expression on the threshold for mitochondrial outer membrane permeabilization (MOMP). The initiation of

Figure 6.

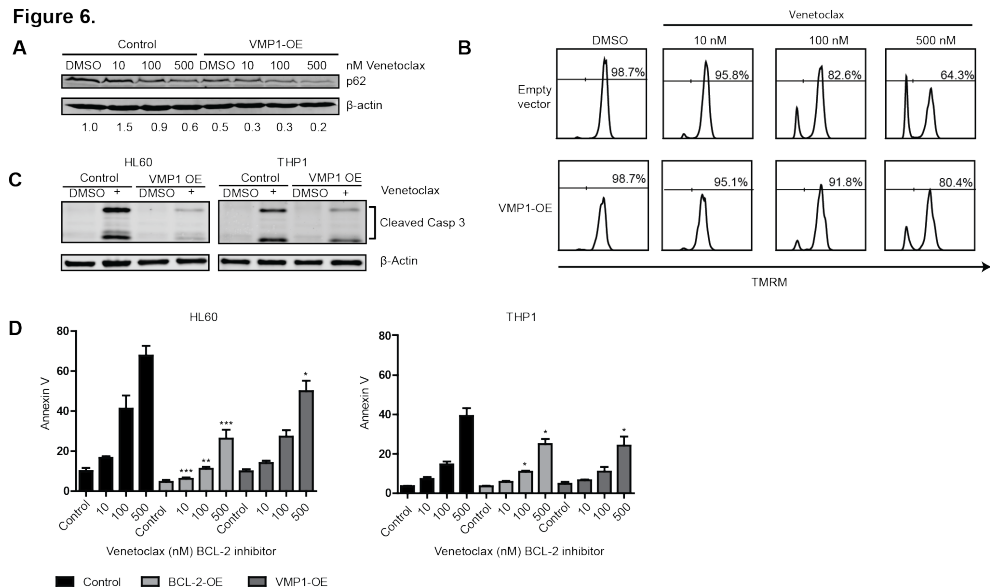


Figure 6. Overexpression of VMP1 interferes with venetoclax induced apoptosis. **A)** Western blot of p62 in THP1 cells overexpressing VMP1 or control treated with different concentrations of venetoclax, beta-actin was used as control. (n=2) **B)** HL60 cells overexpressing VMP1 or control were incubated for 24 hrs with different concentrations of venetoclax. FACS plots show the percentage of TMRM positive cells **C)** Western Blot showing cleaved caspase 3 in HL60 and THP1 cells overexpressing VMP1 or control after 24 hour incubation with 25 nM venetoclax (n=2). **D)** Leukemic cell lines with lentiviral overexpression of VMP1, BCL-2 or control were treated 24 hrs with venetoclax and apoptosis was measured by annexin-V staining with FACS (n=4). Error bars represent SD; *, ** or *** represents $p < .05$, $p < .01$ or $p < .001$, respectively.

MOMP is preceded by loss of mitochondrial membrane potential (MMP) and results in caspase-dependent apoptosis (37). Leukemic cells overexpressing either BCL-2 or VMP1 were treated with increasing concentrations of venetoclax and the MMP was determined after tetramethylrhodamine (TMRM) staining in the context of BCL-2 and VMP1 overexpression. Venetoclax-induced loss of MMP could be partially rescued by VMP1 or BCL-2 overexpression (**Figure 6B** and **Supplemental Figure S5A**). In addition, venetoclax induced apoptotic response in HL60 and THP1 cells, as determined by caspase-3 cleavage and annexin-V staining, could partially be rescued by overexpressing BCL-2 or VMP1 (**Figure 6C-D** and **Supplemental Figure S5B**). To study the specificity of effects, leukemic cell lines were treated with the specific and potent MCL-1 inhibitor S63845 (41). In contrast to BCL-2 overexpression, VMP1 overexpression did not rescue S63845-mediated apoptosis (**Supplemental Figure S5C**). Together, these data indicate that overexpression of BCL-2 and VMP1 increase the threshold for venetoclax-mediated loss of MOMP, thereby reducing apoptosis-mediated cell death.

Discussion

The present study indicates that VMP1 is involved in autophagy and mitochondrial turn-over in normal hematopoietic and leukemic cells. Blocking VMP1 expression impairs the autophagy flux, coinciding with reduced proliferation and survival of normal and leukemic HSPC and impaired *in vivo* engraftment. Previous studies on VMP1 function have been done primarily in solid tumours (42,43), but gene expression studies in hematopoietic cells showed that VMP1 is differentially expressed in hematopoietic cell lineages, including HSPCs. In the leukemic counterpart, VMP1 can be overexpressed in all AML subcategories independent of the molecular and genetic makeup. Functional studies have shown that VMP1 disrupts the binding of BCL-2 to Beclin-1 and consequently de-represses autophagy (23). These findings are in line with our results showing that reduced VMP1 expression resulted in inhibition of autophagy, while overexpression enhanced autophagy-flux. This would also suggest that AMLs with high VMP1 expression are primed for robust autophagy activation in response to cellular stress. In addition, our study showed that high VMP1 expression is inversely correlated with genes enriched for the GO-terms associated with mitochondria, which is in line with studies in Hela cells showing that VMP1 co-localizes with mitochondrial structures (36,39). Based on functional studies and electron microscopy, our results suggest that VMP1 regulates mitochondria quantity and

quality by affecting mitophagy. Higher VMP1 expression reduces mitochondrial copy number and TOM20 expression and increases mitochondrial membrane potential and ATP production. This is indicative for improvement in quality of the remaining mitochondria, while reduced VMP1 expression generated the opposite results. In addition, knockdown of VMP1 resulted in swollen mitochondria and increased ROS levels, which is most likely the consequence of accumulating (dysfunction) mitochondria. Previous studies with ATG12, ATG5 or ATG7 knockout mice have reported comparable results: accumulating dysfunctional mitochondria and ROS (5,44-46).

The higher expression of VMP1 in AML CD34⁺ cells might be protective for AML cells in the hypoxic bone marrow micro-environment, where control of mitochondria content and ROS production by autophagy is crucial for maintaining an immature phenotype (5). Similar to other pro-autophagy genes (47), VMP1 expression can be upregulated under hypoxia (48). However, in leukemic cell lines TOM20 and VMP1 protein levels both declined when the cells were cultured under hypoxia (data not shown). Therefore it is more likely that the mitochondrial turnover during hypoxia is controlled by BNIP3 and BNIP3-L which demonstrate a strong upregulation in response to hypoxia exposure (47).

The threshold for MOMP, and consequently for cytochrome-c release-dependent caspase activation, is regulated by the expression level of BCL-2 protein family members, which might account for drug resistance in a subgroup of AML patients (49-52). Recently, promising results have been obtained with venetoclax in relapsing AML patients in conjunction with low-dose chemotherapy (53). Predictive markers have been identified for reduced sensitivity for venetoclax, such as increased expression of BCL-XL or MCL-1 (41,49,54,55). The present study indicates that VMP1 overexpression is an additional predictive maker for resistance against venetoclax in AML. VMP1 overexpression resulted in an increase in MMP, which could in turn increase the threshold for venetoclax-mediated apoptosis. Mitochondria play a central role in regulation of apoptosis (56). Cells with more mitochondrial content were shown to be more prone to undergo apoptosis (57). Therefore, VMP1 overexpression could potentially inhibit pro-apoptotic signalling by increased turnover of dysfunctional mitochondria. In addition, cells with high VMP1 expression might be primed for a robust autophagy induction in response to venetoclax-mediated de-repression of autophagy, which can contribute to additional chemotherapy resistance.

In summary, the results demonstrate that VMP1 is essential for HSPC and AML cells and is involved in mitochondrial quality control. High VMP1 expression is protective against loss of membrane potential and apoptosis induced by venetoclax.

Conflict of Interest Disclosure

The authors indicate no potential conflict of interests

Acknowledgements

We kindly thank Prof. Robert E. Campbell (Department of Chemistry, University of Alberta, Edmonton, Alberta, Canada) for providing the mBlueberry Fluorescent Protein. In addition, we would like to thank Dr. Tom van Meerten for providing venetoclax and Mylène Gerritsen for help with cloning the BCL-2-OE and VMP1-OE vectors. We would like to thank Anouk H.G. Wolters for technical assistance with the sample preparations for electron microscopy analysis. Finally, we would like to thank Eva van den Berg and André B. Mulder for cytogenetic and mutation analysis of AML patient samples. Part of the work was performed at the UMCG Microscopy and Imaging Center (UMIC) using the Zeiss Supra55 ATLAS, funded by ZonMW grant 91111.006. This research project was supported by a grant of the Dutch Cancer Foundation (KWF, 2010-4771).

Authorship contributions

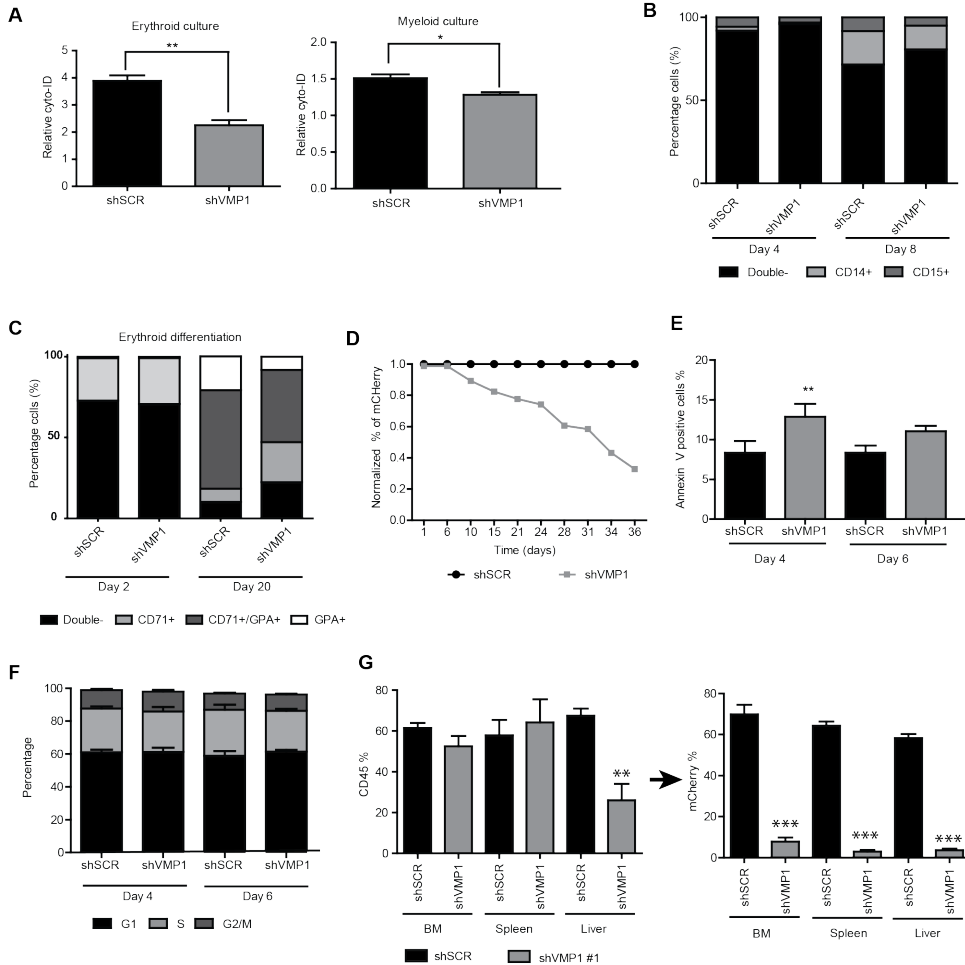
H.F.: conception and design, collection and/or assembly of data, data analysis and interpretation, and manuscript writing. A.T.J.W and F.A.J.v.d.H.: data analysis and interpretation; J.J.S and E.V.: conception and design, data analysis and interpretation, financial support, administrative support, final approval of manuscript; H.F., A.T.J.W., J.J.S. and E.V. conceived and designed the experiments; H.F., F.A.J.v.d.H., R.R.W, D.S.K. and J.J. performed the experiments; H.F., A.T.J.W., J.J.S. and E.V. analyzed the data; H.F, J.J.S. and E.V. wrote the paper.

References

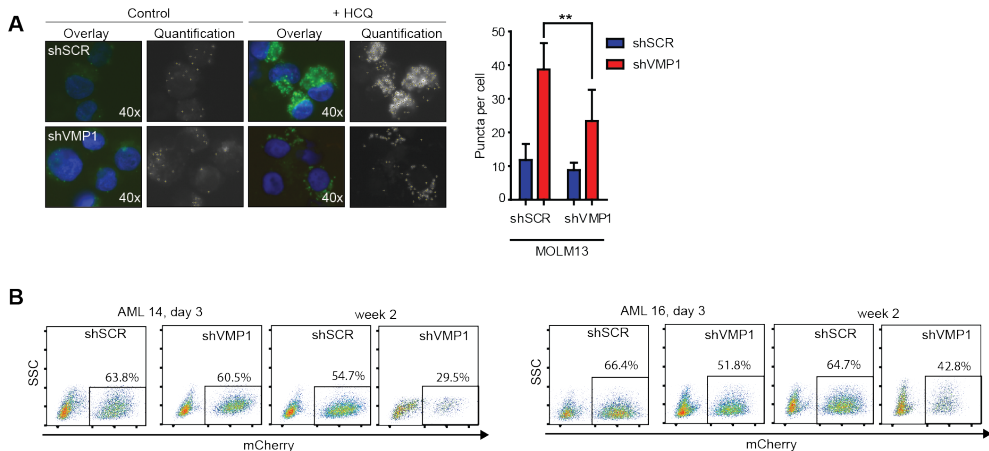
- Luo C, Li Y, Wang H, Feng Z, Long J, Liu J. Mitochondrial accumulation under oxidative stress is due to defects in autophagy. *J Cell Biochem* 2013;114:212-9
- Joshi A, Kundu M. Mitophagy in hematopoietic stem cells: the case for exploration. *Autophagy* 2013;9:1737-4
- Yang Z, Klionsky DJ. Eaten alive: a history of macroautophagy. *Nat Cell Biol* 2010;12:814-22
- Leveque-El Mouttie L, Vu T, Lineburg KE, Kuns RD, Bagger FO, Teal BE, et al. Autophagy is required for stem cell mobilization by G-CSF. *Blood* 2015;125:2933-6
- Ho TT, Warr MR, Adelman ER, Lansinger OM, Flach J, Verovskaya EV, et al. Autophagy maintains the metabolism and function of young and old stem cells. *Nature* 2017;543:205-10
- Gomez-Puerto MC, Folkerts H, Wierenga AT, Schepers K, Schuringa JJ, Coffey PJ, et al. Autophagy Proteins ATG5 and ATG7 Are Essential for the Maintenance of Human CD34(+) Hematopoietic Stem-Progenitor Cells. *Stem Cells* 2016;34:1651-63
- Zhang Y, Morgan MJ, Chen K, Choksi S, Liu ZG. Induction of autophagy is essential for monocyte-macrophage differentiation. *Blood* 2012;119:2895-905
- Kundu M, Lindsten T, Yang CY, Wu J, Zhao F, Zhang J, et al. Ulk1 plays a critical role in the autophagic clearance of mitochondria and ribosomes during reticulocyte maturation. *Blood* 2008;112:1493-502
- Betin VM, Singleton BK, Parsons SF, Anstee DJ, Lane JD. Autophagy facilitates organelle clearance during differentiation of human erythroblasts: evidence for a role for ATG4 paralogs during autophagosome maturation. *Autophagy* 2013;9:881-93
- Zhang J, Randall MS, Loyd MR, Dorsey FC, Kundu M, Cleveland JL, et al. Mitochondrial clearance is regulated by Atg7-dependent and -independent mechanisms during reticulocyte maturation. *Blood* 2009;114:157-64
- Folkerts H, Hilgendorf S, Wierenga ATJ, Jaques J, Mulder AB, Coffey PJ, et al. Inhibition of autophagy as a treatment strategy for p53 wild-type acute myeloid leukemia. *Cell Death Dis* 2017;8:e2927
- Man N, Tan Y, Sun XJ, Liu F, Cheng G, Greenblatt SM, et al. Caspase-3 controls AML1-ETO-driven leukemogenesis via autophagy modulation in a ULK1-dependent manner. *Blood* 2017;129:2782-92
- Rudat S, Pfaus A, Cheng YY, Holtmann J, Ellegast JM, Buhler C, et al. RET-mediated autophagy suppression as targetable co-dependence in acute myeloid leukemia. *Leukemia* 2018;2189-202
- Auberger P, Puissant A. Autophagy, a key mechanism of oncogenesis and resistance in leukemia. *Blood* 2017;129:547-52
- Piya S, Kornblau SM, Ruvolo VR, Mu H, Ruvolo PP, McQueen T, et al. Atg7 suppression enhances chemotherapeutic agent sensitivity and overcomes stroma-mediated chemoresistance in acute myeloid leukemia. *Blood* 2016;128:1260-9
- Sumitomo Y, Koya J, Nakazaki K, Kataoka K, Tsuruta-Kishino T, Morita K, et al. Cytoprotective autophagy maintains leukemia-initiating cells in murine myeloid leukemia. *Blood* 2016;128:1614-24
- Stankov MV, El Khatib M, Kumar Thakur B, Heitmann K, Panayotova-Dimitrova D, Schoening J, et al. Histone deacetylase inhibitors induce apoptosis in myeloid leukemia by suppressing autophagy. *Leukemia* 2014;28:577-88
- Altman JK, Szilard A, Goussetis DJ, Sassano A, Colamonic M, Gounaris E, et al. Autophagy is a survival mechanism of acute myelogenous leukemia precursors during dual mTORC2/mTORC1 targeting. *Clin Cancer Res* 2014;20:2400-9
- Visconte V, Przychodzen B, Han Y, Nawrocki ST, Thota S, Kelly KR, et al. Complete mutational spectrum of the autophagy interactome: a novel class of tumor suppressor genes in myeloid neoplasms. *Leukemia* 2017;31:505-10
- Liu Q, Chen L, Atkinson JM, Claxton DF, Wang HG. Atg5-dependent autophagy contributes to the development of acute myeloid leukemia in an MLL-AF9-driven mouse model. *Cell Death Dis* 2016;7:e2361
- Zhao YG, Chen Y, Miao G, Zhao H, Ou W, Li D, et al. The ER-Localized Transmembrane Protein EPG-3/VMP1 Regulates SERCA Activity to Control ER-Isolation Membrane Contacts for Autophagosome Formation. *Mol Cell* 2017;67:974-89
- Nascimbeni AC, Giordano F, Dupont N, Grasso D, Vaccaro MI, Codogno P, et al. ER-plasma membrane contact sites contribute to autophagosome biogenesis by regulation of local PI3P synthesis. *EMBO J* 2017;36:2018-33
- Molejon MI, Ropolo A, Vaccaro MI. VMP1 is a new player in the regulation of the autophagy-specific phosphatidylinositol 3-kinase complex activation. *Autophagy* 2013;9:933-5
- Erlich S, Mizrachy L, Segev O, Lindenboim L, Zmira O, Adi-Harel S, et al. Differential interactions between Beclin 1 and Bcl-2 family members. *Autophagy* 2007;3:561-8
- Guo L, Yang LY, Fan C, Chen GD, Wu F. Novel roles of Vmp1: inhibition metastasis and proliferation of hepatocellular carcinoma. *Cancer Sci* 2012;103:2110-9
- Ropolo A, Grasso D, Pardo R, Sacchetti ML, Archange C, Lo Re A, et al. The pancreatitis-induced vacuole membrane protein 1 triggers autophagy in mammalian cells. *J Biol Chem* 2007;282:37124-33
- van Gosliga D, Schepers H, Rizo A, van der Kolk D, Vellenga E, Schuringa JJ. Establishing long-term cultures with self-renewing acute myeloid leukemia stem/progenitor cells. *Exp Hematol* 2007;35:1538-49
- Rooney JP, Ryde IT, Sanders LH, Howlett EH, Colton MD, Germ KE, et al. PCR based determination of mitochondrial DNA copy number in multiple species. *Methods Mol Biol* 2015;1241:23-38
- de Jonge HJ, Valk PJ, Veeger NJ, ter Elst A, den Boer ML, Cloos J, et al. High VEGFC expression is associated with unique gene expression profiles and predicts adverse prognosis in pediatric and adult acute myeloid leukemia. *Blood* 2010;116:1747-54
- Ley TJ, Miller C, Ding L, Raphael BJ, Mungall AJ, Robertson A, et al. Genomic and epigenomic landscapes of adult de novo acute myeloid leukemia. *N Engl J Med* 2013;368:2059-74
- Huang da W, Sherman BT, Lempicki RA. Bioinformatics enrichment tools: paths toward the comprehensive functional analysis of large gene lists. *Nucleic Acids Res* 2009;37:1-13

32. Houwerzijl EJ, Blom NR, van der Want JJ, Louwes H, Esselink MT, Smit JW, et al. Increased peripheral platelet destruction and caspase-3-independent programmed cell death of bone marrow megakaryocytes in myelodysplastic patients. *Blood* 2005;105:3472-9
33. Carper D, Smith-Gill SJ, Kinoshita JH. Immunocytochemical localization of the 27K beta-crystallin polypeptide in the mouse lens during development using a specific monoclonal antibody: implications for cataract formation in the Philly mouse. *Dev Biol* 1986;113:104-9
34. Bagger FO, Sasivarevic D, Sohi SH, Laursen LG, Pundhir S, Sonderby CK, et al. BloodSpot: a database of gene expression profiles and transcriptional programs for healthy and malignant haematopoiesis. *Nucleic Acids Res* 2016;44:917-24
35. Klionsky DJ, Abdelmohsen K, Abe A, Abedin MJ, Abeliovich H, Acevedo Arozena A, et al. Guidelines for the use and interpretation of assays for monitoring autophagy (3rd edition). *Autophagy* 2016;12:1-222
36. Tabara LC, Escalante R. VMP1 Establishes ER-Microdomains that Regulate Membrane Contact Sites and Autophagy. *PLoS One* 2016;11:e0166499
37. Czabotar PE, Lessene G, Strasser A, Adams JM. Control of apoptosis by the BCL-2 protein family: implications for physiology and therapy. *Nat Rev Mol Cell Biol* 2014;15:49-63
38. Molejon MI, Ropolo A, Re AL, Boggio V, Vaccaro MI. The VMP1-Beclin 1 interaction regulates autophagy induction. *Sci Rep* 2013;3:1055
39. Chiang WC, Wei Y, Kuo YC, Wei S, Zhou A, Zou Z, et al. High-Throughput Screens To Identify Autophagy Inducers That Function by Disrupting Beclin 1/Bcl-2 Binding. *ACS Chem Biol* 2018;13:2247-60
40. Bodo J, Zhao X, Durkin L, Souers AJ, Phillips DC, Smith MR, et al. Acquired resistance to venetoclax (ABT-199) in t(14;18) positive lymphoma cells. *Oncotarget* 2016;7:70000-10
41. Kotschy A, Szlavik Z, Murray J, Davidsen J, Maragno AL, Le Toumelin-Braizat G, et al. The MCL1 inhibitor S63845 is tolerable and effective in diverse cancer models. *Nature* 2016;538:477-82
42. Zheng L, Chen L, Zhang X, Zhan J, Chen J. TMEM49-related apoptosis and metastasis in ovarian cancer and regulated cell death. *Mol Cell Biochem* 2016;416:1-9
43. Loncle C, Molejon MI, Lac S, Tellechea JI, Lomberk G, Gramatica L, et al. The pancreatitis-associated protein VMP1, a key regulator of inducible autophagy, promotes Kras(G12D)-mediated pancreatic cancer initiation. *Cell Death Dis* 2016;7:e2295
44. Mortensen M, Soilleux EJ, Djordjevic G, Tripp R, Lutteropp M, Sadighi-Akha E, et al. The autophagy protein Atg7 is essential for hematopoietic stem cell maintenance. *J Exp Med* 2011;208:455-67
45. Stephenson LM, Miller BC, Ng A, Eisenberg J, Zhao Z, Cadwell K, et al. Identification of Atg5-dependent transcriptional changes and increases in mitochondrial mass in Atg5-deficient T lymphocytes. *Autophagy* 2009;5:625-35
46. Liang CC, Wang C, Peng X, Gan B, Guan JL. Neural-specific deletion of FIP200 leads to cerebellar degeneration caused by increased neuronal death and axon degeneration. *J Biol Chem* 2010;285:3499-509
47. Bellot G, Garcia-Medina R, Gounon P, Chiche J, Roux D, Pouyssegur J, et al. Hypoxia-induced autophagy is mediated through hypoxia-inducible factor induction of BNIP3 and BNIP3L via their BH3 domains. *Mol Cell Biol* 2009;29:2570-581
48. Rodriguez ME, Catrinacio C, Ropolo A, Rivarola VA, Vaccaro MI. A novel HIF-1alpha/VMP1-autophagic pathway induces resistance to photodynamic therapy in colon cancer cells. *Photochem Photobiol Sci* 2017;16:1631-42
49. Valentin R, Grabow S, Davids MS. The rise of apoptosis: targeting apoptosis in hematologic malignancies. *Blood* 2018;132:1248-64
50. Bosman MC, Schepers H, Jaques J, Brouwers-Vos AZ, Quax WJ, Schuringa JJ, et al. The TAK1-NF-kappaB axis as therapeutic target for AML. *Blood* 2014;124:3130-40
51. Jilg S, Reidel V, Muller-Thomas C, Konig J, Schauwecker J, Hockendorf U, et al. Blockade of BCL-2 proteins efficiently induces apoptosis in progenitor cells of high-risk myelodysplastic syndromes patients. *Leukemia* 2016;30:112-23
52. Mehta SV, Shukla SN, Vora HH. Overexpression of Bcl2 protein predicts chemoresistance in acute myeloid leukemia: its correlation with FLT3. *Neoplasma* 2013;60:666-75
53. Liu B, Narurkar R, Hanmantgad M, Zafar W, Song Y, Liu D. Venetoclax and low-dose cytarabine induced complete remission in a patient with high-risk acute myeloid leukemia: a case report. *Front Med* 2018;Epub ahead of print
54. Pan R, Hogdal LJ, Benito JM, Buccì D, Han L, Borthakur G, et al. Selective BCL-2 inhibition by ABT-199 causes on-target cell death in acute myeloid leukemia. *Cancer Discov* 2014;4:362-75
55. Konopleva M, Pollyea DA, Potluri J, Chyla B, Hogdal L, Busman T, et al. Efficacy and Biological Correlates of Response in a Phase II Study of Venetoclax Monotherapy in Patients with Acute Myelogenous Leukemia. *Cancer Discov* 2016;6:1106-17
56. Sriskanthadevan S, Jeyaraju DV, Chung TE, Prabha S, Xu W, Skrtic M, et al. AML cells have low spare reserve capacity in their respiratory chain that renders them susceptible to oxidative metabolic stress. *Blood* 2015;125:2120-30
57. Marquez-Jurado S, Diaz-Colunga J, das Neves RP, Martinez-Lorente A, Almazan F, Guantes R, et al. Mitochondrial levels determine variability in cell death by modulating apoptotic gene expression. *Nat Commun* 2018;9:389

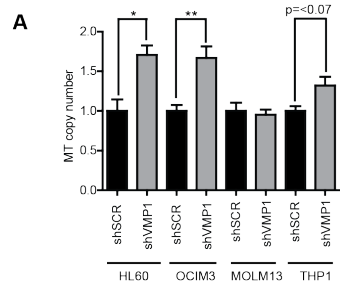
Supplementary Figures



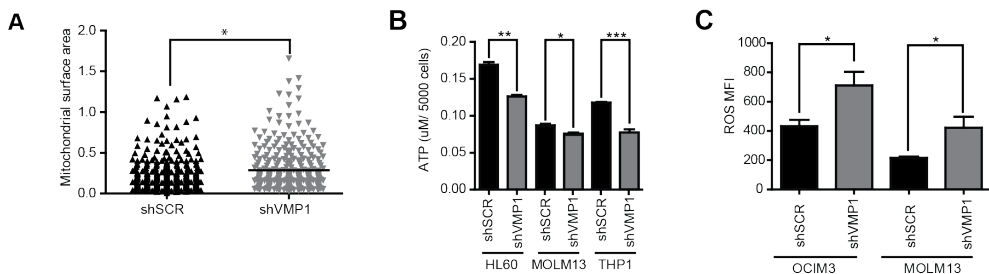
Supplementary Figure S1 VMP1 knockdown results impaired expansion and increased apoptosis in leukemic cells. A) Relative Cyto-ID MFI in shSCR and shVMP1 transduced cord blood (CB) CD34⁺ cultured under erythroid or myeloid permissive conditions and treated overnight with or without HCQ. B-C) Representative percentages of myeloid differentiation markers CD14 and CD15 or erythroid differentiation makers CD71 and GPA in time of shSCR and shVMP1 transduced CB CD34⁺ cells (n=2). D) Representative graph showing the percentage of mCherry positive cells in an MS5 coculture of unsorted CD34⁺ cells, transduced with shSCR-mCherry or shVMP1-mCherry (n=2). E-F) Annexin-V percentage and cell cycle distribution of shSCR or shVMP1 transduced CB CD34⁺ cells at day 4 and 6 after transduction (n=3). G) Engraftment (percentage huCD45) at time of sacrifice in bone marrow, spleen and liver (left graph) and the mCherry percentage within the huCD45⁺ population (right graph). Error bars represent SD; *, ** or *** represents $p < .05$, $p < .01$ or $p < .001$, respectively.



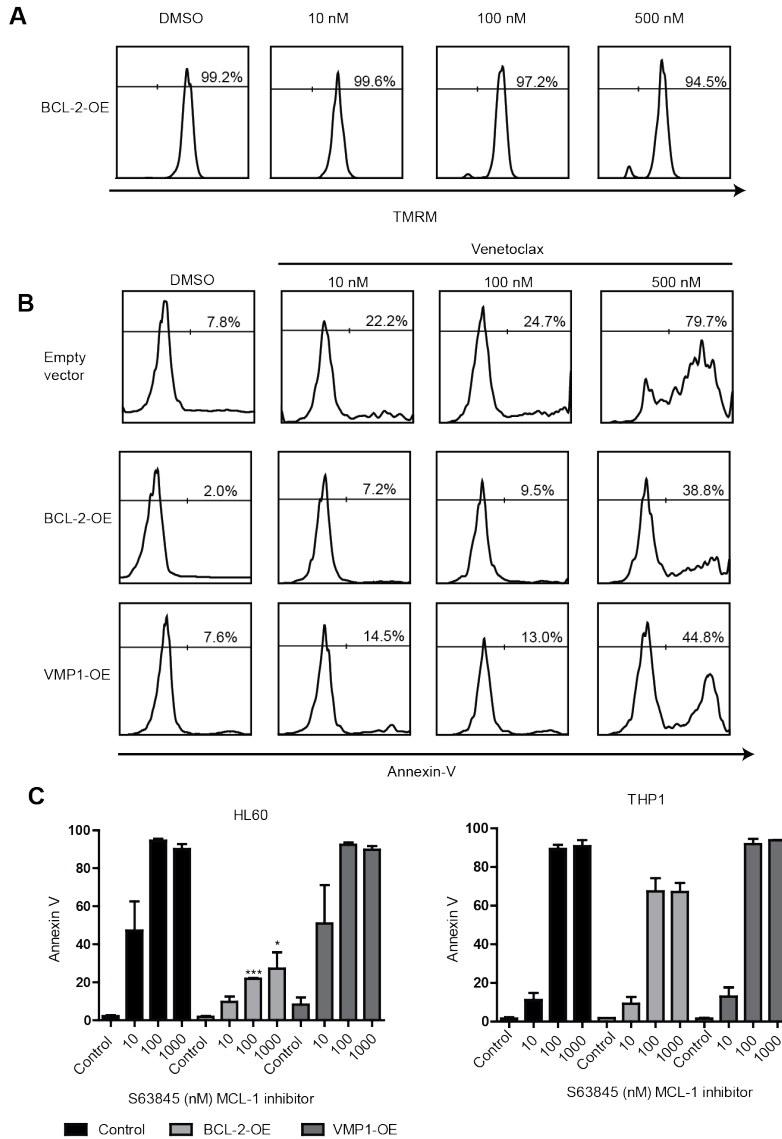
Supplemental Figure S2: VMP1 knockdown results impaired expansion and increased apoptosis in leukemic cells. A). Left panel, representative pictures showing GFP-LC3 puncta in shSCR or shVMP1 transduced MOLM13 cells treated with or without HCQ. Right panel, quantification of LC3 puncta. B) Representative FACS plots of shSCR-mCherry or shVMP1-mCherry transduced primary AML CD34+ cells at day 3 and after 2 weeks.



Supplemental Figure S3: Overexpression of VMP1 increases autophagic flux in leukemic cells and is involved in mitochondrial turnover. A) Mitochondrial copy number in leukemic cell lines transduced with shSCR or shVMP1 after 3 days of knockdown.



Supplemental Figure S4: Ultrastructural analysis of OCIM3 cells after VMP1 modulation. A) Electron microscopy analysis of total mitochondrial surface area in OCIM3 cells transduced with shSCR or shVMP1 (n=324 mitochondria per group). B) ATP levels, measured in leukemic cell lines transduced with shSCR or shVMP1. C) FACS analysis of CellROX (ROS) MFI in leukemic cell lines cells transduced with shSCR or shVMP1. Error bars represent SD; *, ** or *** represents p < .05, p < .01 or p < .001, respectively.



Supplemental Figure S5: Overexpression of VMP1 interferes with venetoclax induced apoptosis in leukemic cells. A-B) HL60 cells overexpressing BCL-2, VMP1 or control were incubated for 24 hrs with different concentrations of venetoclax. FACS plots show the percentage of tetramethylrhodamine (TMRM) positive or annexin-V positive cells with increasing concentrations of venetoclax. **C)** Leukemic cell lines with lentiviral overexpression of VMP1, BCL-2 or control were treated 24 hrs with MCL-1 inhibitor S63845 and apoptosis was measured after annexin-V staining with FACS (n=4).

